IEEE Access
Multidisciplinary ⋮ Rapid Review ⋮ Open Access Journal

Date of publication xxxx 00, 0000, date of current version xxxx 00, 0000.

*Digital Object Identifier 10.1109/ACCESS.2017.DOI*

# Challenges and Opportunities in Wireless Fronthaul

**DAVE TOWNEND[1], RYAN HUSBANDS[2], STUART D.WALKER[3], ANDY SUTTON[4]**

[1]BT Labs, Adastral Park, Martlesham, UK (e-mail: dave.townend@bt.com)
[2]BT Labs, Adastral Park, Martlesham, UK (e-mail: ryan.husbands@bt.com)
[3]University of Essex, Wivenhoe Park, Colchester, UK (e-mail: stuwal@essex.ac.uk)
[4]BT Technology, London, UK (e-mail: andy.sutton@bt.com)

Corresponding author: Dave Townend (e-mail: dave.townend@bt.com).

## ABSTRACT

To date the evolution from traditional distributed radio access networks (D-RAN) towards fronthaul oriented centralized (C-RAN) architectures has imposed significant challenges for the underlying transport network. The processing and coordination benefits anticipated in C-RAN are generally underpinned with the assumption of a full fiber transport network capable of meeting the demanding performance criteria of fronthaul transport. Recent advances in Ethernet based fronthaul interfaces together with exploration of new mmWave and sub-THz spectrum bands present an opportunity for wireless solutions to also realize these fronthaul transport requirements. In this work, the requirements for promising new Ethernet based fronthaul interfaces are explored. These requirements are assessed against the measured capabilities of a state-of-the-art E-band (71-86 GHz) wireless transport solution. The experimental results are then used to forecast the performance expectations of future higher bandwidth systems operating above 100 GHz. A dimensioning and link budget analysis is performed for the various candidate spectrum bands and fronthaul interfaces to highlight the viability of fronthaul delivered over wireless transport. Finding show that transport solutions operating at mmWave and sub-THz frequencies are able to support the performance requirements of newly standardized fronthaul interface splits and as such present an opportunity to utilize wireless fronthaul transport in C-RAN architectures where fiber cannot otherwise be supported. Furthermore, analysis demonstrates that the hop lengths possible for 5G small cell configurations are well aligned with the expected inter-site distances of future dense urban cell deployments making wireless fronthaul a promising concept for realizing future C-RAN based cell densification.

**INDEX TERMS** Wireless fronthaul, C-RAN, mmWave, x-haul, D-band

## I. INTRODUCTION

THE use of wireless transport in radio access network (RAN) cell site deployments is a well established approach to backhaul provisioning. The use of wireless backhaul is generally favored where fiber optic connectivity is either absent or cost prohibitive. In fact, wireless transport solutions such as point-to-point microwave account for the majority of existing cell site backhaul installations worldwide [25].

The use of fixed-service microwave bands (6-42 GHz) by operators and infrastructure providers has proven well aligned with the backhaul requirements of 3G and 4G RAN deployments to date. However, the introduction of higher capacity 5G RAN and an architectural evolution towards disaggregated and centralized deployment models bring new performance challenges for wire-

less transport systems [24]. This evolution brings about three transport categories known as backhaul, midhaul and fronthaul which are collectively referred to as 'x-haul'. To address these new x-haul challenges, the next generation wireless transport solutions must target new performance criteria suitable of offering a viable alternative to fiber. In response, a migration to millimeter-wave transmission bands, such as W-band (92-114.25 GHz) and D-band (130-174.8 GHz) [16] is being considered for future high capacity, low latency wireless x-haul scenarios [24].

Underpinning the new requirements placed on wireless transport is the specification of new 'functional splits' in 5G standards which aim to increase deployment flexibility of the RAN. Moreover, the adoption of alternative functional splits further facilitates the realization of centralized and virtualized radio access network (C-RAN /vRAN) components [50, 47]. Functional splits allow for geographic separation and disaggregation of the traditional RAN cell site functions throughout the network [38, 41]. In such architectures, the radio unit (RU) is principally concerned with radio signal reception and transmission at the cell site whilst real-time signaling procedures are handled by the distributed unit (DU) and non-real-time higher layer protocol functions handled by the centralized unit (CU). C-RAN architectures are able to support a range of new deployment scenarios from consolidation and disaggregation of baseband capabilities to more efficient cell densification. Such architectures however, each necessitate new high capacity, low latency fronthaul based transport interfaces. As such the challenge for wireless transport is whether it can meet the performance and deployment requirements necessary to support C-RAN architectures.

### A. RELATED WORKS

In recent years the theoretical requirements for fronthaul based transport interfaces have been well studied [38, 41]. Whilst each split point in the 5G protocol stack may be suited to a particular deployment scenario, the impact of the associated performance requirements are not well studied beyond the optical transport domain. Historically, it has been assumed that the benefits of C-RAN architectures could only realistically be achieved using large scale fiber transport networks [28]. As such fronthaul and C-RAN challenges for a wide range optical transport technologies including Passive Optical Networks (PON) and Wavelength Division Multiplexing (WDM) have been extensively studied [9] including the use of free space optics (FSO). It is however recognized that although technologies such as FSO alleviate some of the inherent inflexibility of fiber transport in the same way a radio, they also pose significant atmospheric availability challenges which in turn has resulted in research effort into optimization of hybrid FSO and radio solutions for fronthaul networks [29].

Some studies considering the performance criteria of fronthaul interfaces have however been considered for wireless transport from a theoretical perspective. In [36] and [17] a number of promising enabling technologies such as fronthaul compression and line-of-sight MIMO are considered as a means of meeting fronthaul performance criteria with wireless transport. Analysis suggests that reliable fronthaul performance can be achieved using line-of-sight MIMO at 80 GHz in order to meet the necessary spectral efficiency. In [37] it is recognized that the flexibility of wireless transport solutions offer cost and time benefits over the more ideal optical transport. A number of candidate mmWave bands are also explored where it is concluded that the requirements of upper-layer fronthaul split interfaces could be met with existing bands below 100 GHz whilst suggesting lower layer splits would need to be addressed with higher capacity spectrum bands above 100 GHz due to the more demanding latency requirements. The data rate requirements of various fronthaul splits are also calculated for a range of realistic 5G cell configurations in [44]. Here, the data rate requirements are compared with simulation results of the available capacity from various channel bandwidths operating at 105 GHz and 220 GHz sub-THz bands. Results suggest that option 8 and 7.1 splits are not a suitable split option for sub-THz fronthaul transport where link distance of least 100 m is required.

Further to the theoretical support, experimental studies based on proprietary wireless transport solutions in [42] have also demonstrated the latency requirements of low layer fronthaul splits could

be met using 60 GHz and 70 GHz radio solutions. A wireless fronthaul proof of concept based on the most challenging option 8 split has also been studied using E-band (71-86 GHz) point-to-point transport in [48]. Results in this study have demonstrated the performance requirements for fronthaul interfaces can be met with existing wireless transport solutions albeit for basic low capacity cell configurations.

While literature to date suggests the concept of wireless fronthaul could be realized to some extent both theoretically and experimentally, research has generally been focused specifically on data rates or latency key performance indicators (KPIs). Studies have stopped short in considering all fronthaul performance criteria for specific fronthaul interfaces when applied to spectrum bands with industry and standardization traction. To address literature gaps and understand the viability of wireless fronthaul, a wider analysis is required supported by real-world performance measurements more representative of commercial deployments. As Ethernet based fronthaul interfaces start to become a reality due to standardization efforts (at various split points highlighted in Fig.1) from industry forums such as eCPRI [21], O-RAN [39] and Small Cell Forum (SCF) [45], the question of wireless fronthaul viability also becomes more evident and whether there is an opportunity for emerging wireless transport solutions to accelerate the adoption of commercial C-RAN deployments.

### B. CONTRIBUTIONS AND ORGANIZATION

In this study, we consider the fundamental requirements of emerging fronthaul interfaces at key functional split points (options 8, 7.2 and 6). These are contrasted with the performance characteristics of mmWave and sub-THz wireless transport bands (E, W and D band). The resulting analysis contributes fronthaul requirement dimensioning of representative 5G small cell configurations together with the necessary performance KPI predictions needed to meet them using wireless transmission. These contributions aim to provide new insight into the feasibly of deploying 5G small cells in environments such as urban street canyons using wireless fronthaul. Crucially, analysis is based on industry standardized fronthaul interfaces and spectrum bands targeted for global harmonization.

The key challenges to wireless fronthaul are addressed in the context of the theoretical requirements of Ethernet based fronthaul interfaces in Section II. An experimental test bed is presented in Section III where the performance capability of an E-band point-to-point link is measured and used to extrapolate the anticipated performance of future higher bandwidth systems above 100 GHz. These performance characteristics are subsequently compared with the fronthaul interface requirements of a representative 5G small cell RU. The deployment opportunity for wireless fronthaul is presented in Section IV where the anticipated operational link budget and performance of candidate wireless fronthaul transport bands is derived. This is subsequently combined in a dimensioning exercise with the various fronthaul interface requirements. Finally, results are discussed in Section V with the aim of highlighting the potential of high frequency transport bands to deliver candidate fronthaul interfaces splits over wireless transport.

## II. FRONTHAUL REQUIREMENT CHALLENGES

Although historically the relative merits of all 3GPP split points have considered [18], [38],[11], only splits with established industry traction are considered in the following analysis. The generalized requirements of fronthaul splits (below the MAC layer) can be summarized in terms of data rate, latency, jitter and frame loss. These KPIs represent the performance criteria which a wireless transport solution must overcome in order to support fronthaul interfaces and offer a credible alternative to fiber.

### A. DATA RATE

#### 1) Option 8 Split

The 3GPP option 8 split, whilst offering the lowest complexity RU and highest potential centralization gains requires the most demanding transport data rate [19]. The radio interface I/Q is sampled and quantized resulting in a constant bit rate interface which scales with number of antennas and channel bandwidth (FFT size). The PHY/RF option 8 split as specified in 3GPP TR 38.801

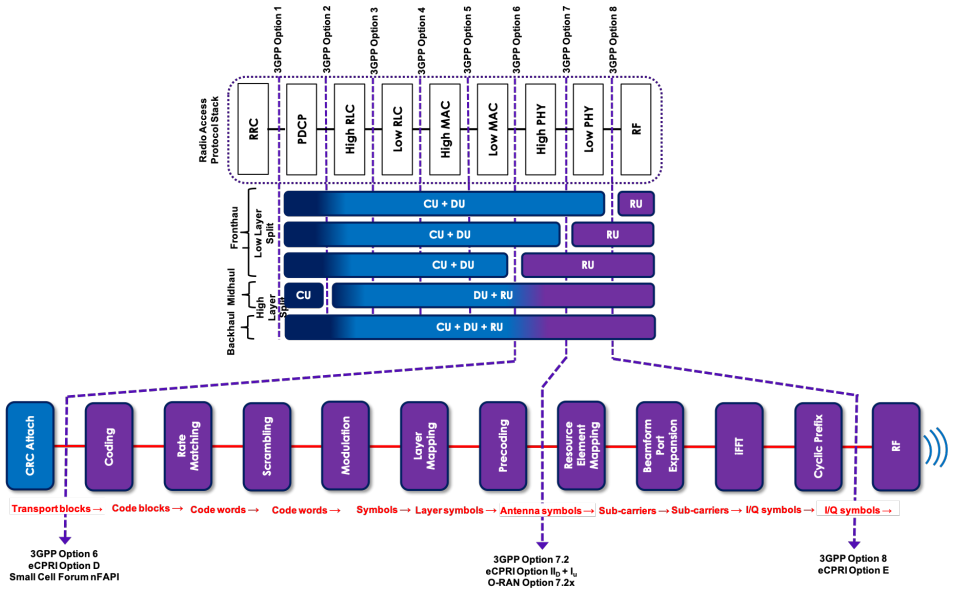


FIGURE 1: RAN Functional Split Overview.

has conventionally been addressed with the CPRI (Common Public Radio Interface) implementation [20] necessitating dedicated fiber optic transport. The evolutionary trend towards more cost effective Ethernet based fronthaul however, now make this split realizable with carrier grade Ethernet solutions such as eCPRI split E [21] or IEEE 1914.3 Radio over Ethernet (RoE) [31] encapsulation.

The transport data rate for conventional CPRI $D_{CPRI}$ can be calculated as in (1). Here, $N_{ant}$ is the number of antenna ports on the RU, $fs$ is the sampling frequency - which is the product of the sub-carrier spacing and the FFT size (scaling with bandwidth) and $M$ which is the number of quantizer bits per I and Q (conventionally 15 bit). Additional overheads are included from control and management words per CPRI frame (1/16) $CM_{CPRI}$ and line coding $LC_{CPRI}$ (either 10/8 for 8B/10B or 66/64 for 64B/66B coding for DC balance and clock recovery). For an Ethernet based option 8 split such as eCPRI $D_{eCPRI}$ the line coding is replaced with overheads from Ethernet framing $OH_{ETH}$ and eCPRI header encapsulation $OH_{eCPRI}$ as in (2).

$$D_{CPRI} = N_{ant} \cdot fs \cdot 2M \cdot CM_{CPRI} \cdot LC_{CPRI} \quad (1)$$

$$D_{eCPRI} = N_{ant} \cdot fs \cdot 2M \cdot CM_{CPRI} \cdot OH_{ETH} \cdot OH_{eCPRI} \quad (2)$$

### 2) Option 7.2 Split

The O-RAN 7.2x split is broadly aligned with eCPRI split $II_D$ and $I_U$ where reduction in the required interface bandwidth (relative to Option 8) is achieved through resource element mapping functions remaining within the RU. Whilst this split adds more complexity to the RU, it enables only user occupied resource elements to traverse the fronthaul interface. As a result the 7.2x split is the first split which allows for a variable bit rate interface. This however does require the introduction of control plane overhead $OH_{CP}$ needed to carry the resource block assignment and any antenna beamforming information in the downlink between DU and RU. As the control plane messaging is implementation specific, the data rate requirements for this split can vary between implementations. The O-RAN alliance suggest control plane overhead in the order of 10% [39].

The transport data rate for O-RAN 7.2x implementation $D_{7.2x}$ can be calculated as in (3) and (4) where the uplink and downlink are specified differently due to the lack of control plane overhead $OH_{CP}$ needed in the uplink. At this split,

the transport requirements can be reduced because transport data rates become a function of the MIMO layers $N_{layers}$ in operation as well as the occupied resource block allocation $N_{PRB}$ (where a utilization scaling factor of 1 is assumed for peak data rate requirement). In the 7.2x split, it is assumed that some element of I/Q compression is employed for each resource block, in O-RAN this is specified as a block floating point compression where each subcarrier $N_{SCperRB}$ I and Q samples are compressed to a signed bitwidth $M_{mantissia}$ and unsigned exponent $M_{exponent}$ (typically 9 bit and 4 bit respectively). The underlying L2 and L3 transport protocols for this split also introduce Ethernet framing $OH_{ETH}$ and eCPRI encapsulation $OH_{eCPRI}$ overhead.

$$D_{7.2x_{DL}} = (N_{layers} \cdot N_{PRB}) \cdot (N_{SCperRB} \cdot 2M_{mantissa} + M_{exponent}) \cdot T_{SymPerSlot}^{-1} \cdot OH_{CP} \cdot OH_{ETH} \cdot OH_{eCPRI} \quad (3)$$

$$D_{7.2x_{UL}} = (N_{layers} \cdot N_{PRB}) \cdot (N_{SCperRB} \cdot 2M_{mantissa} + M_{exponent}) \cdot T_{SymPerSlot}^{-1} \cdot OH_{ETH} \cdot OH_{eCPRI} \quad (4)$$

### 3) Option 6 Split

The option 6 split separates the PHY and MAC layer in the protocol stack whereby all PHY related functions are carried out at the RU and the MAC layer and above are controlled at the DU. At this split point, the transport requirements can be reduced further as the fronthaul interface carries only the MAC transport blocks which are a function of the individual channel coding rate and data rate of each user. This also means that relative to the lower layer splits, the option 6 split has a higher proportion of control traffic as the MAC scheduling functions are also transported to the PHY layers at the RU. The most significant standardization efforts for option 6 are driven by the Small Cell Forum where the nFAPI specification targets low cost, small coverage and indoor cell deployments where higher order massive MIMO and advanced transmission schemes are not envisaged. The transport data rate requirement for nFAPI split 6 implementation $D_{6nFAPI}$ can be calculated as in (5) and (6). For a MAC / PHY split the fronthaul data rate requirements are dependent on the number of MIMO layers $N_{layers}$ and Transport Block Size $TBS$ in use which in turn is dictated by the modulation and coding scheme index $I_{MCS}$ being utilized on the radio interface together with the number of scheduled Resource Blocks $N_{PRB}$. For peak fronthaul data rates the maximum cell utilization is assumed at the maximum $MCS$ supported. In 4G LTE the $TBS$ calculation is given by static lookup tables in 3GPP TS 36.213 [2]. For 5G NR the TBS calculation is made using specific formulas as defined 3GPP TS 38.214 [5] to account for the much larger combinations of modulation/coding scheme and resource block allocations possible. The nFAPI specification defines a message API between MAC and PHY layer fronthaul flows and as such includes a nFAPI encapsulated control plane overhead $OH_{CP}$ and an associated L4 transport overhead header $OH_{nFAPI}$ in addition to the necessary L3 IP overhead $OH_{IP}$ and L2 Ethernet framing overhead $OH_{ETH}$.

$$D_{6nFAPI_{LTE}} = N_{layers} \cdot (TBS \cdot N_{TTIperSec}) + OH_{CP} \cdot OH_{ETH} \cdot OH_{IP} \cdot OH_{nFAPI} \quad (5)$$

$$D_{6nFAPI_{NR}} = N_{layers} \cdot (TBS \cdot T_{slot}^{-1}) \cdot OH_{CP} \cdot OH_{ETH} \cdot OH_{IP} \cdot OH_{nFAPI} \quad (6)$$

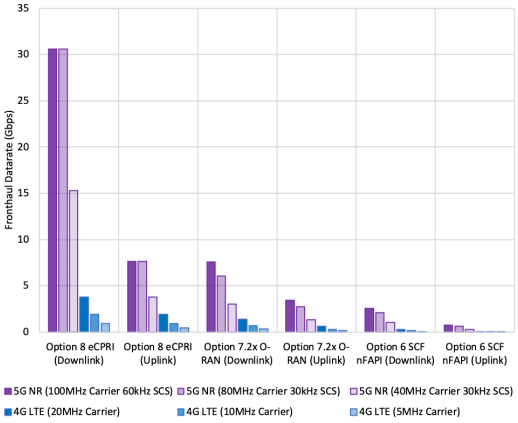


FIGURE 2: Example Fronthaul Data Rates.

An example of the anticipated fronthaul data rates for common cell configurations of a single RU are outlined in Table 1 and shown in Fig. 2. It is important to note further scaling of fronthaul data rates is required for a typical macro cell site which may consist of up to three RU sectors and

TABLE 1: Cell Configuration Used for Fronthaul Data Rate Calculations.

| | 4G LTE | | | 5G NR (FR1) | | |
|---|---|---|---|---|---|---|
| Channel Bandwidth ($MHz$) | 5 | 10 | 20 | 40 | 80 | 100 |
| SC Spacing ($kHz$) | 15 | 15 | 15 | 30 | 30 | 60 |
| SC Per RB [$N_{SCperRB}$] | 12 | 12 | 12 | 12 | 12 | 12 |
| RB Bandwidth ($kHz$) | 180 | 180 | 180 | 360 | 360 | 720 |
| Resource Blocks [$N_{PRB}$] | 25 | 50 | 100 | 107 | 217 | 135 |
| Subcarriers [$N_{SC}$] | 300 | 600 | 1200 | 1284 | 2604 | 1620 |
| Symbols per Slot [$N_{SymPerSlot}$] | 14 | 14 | 14 | 14 | 14 | 14 |
| Slot Length [$T_{slot}$] ($ms$) | 0.001 | 0.001 | 0.001 | 0.0005 | 0.0005 | 0.00025 |
| Sym Period per Slot [$T_{SymPerSlot}$] ($\mu s$) | 71.4 | 71.4 | 71.4 | 35.7 | 35.7 | 17.9 |
| FFT Size | 512 | 1024 | 2048 | 2048 | 4096 | 2048 |
| Sampling Frequency [$fs$] ($MHz$) | 7.68 | 15.36 | 30.72 | 61.44 | 122.88 | 122.88 |
| I/Q Quantizer Bits [$M$] | 15 | 15 | 15 | 15 | 15 | 15 |
| Mantissa Bits [$N_{mantissa}$] | 9 | 9 | 9 | 9 | 9 | 9 |
| Exponent Bits [$N_{exponent}$] | 4 | 4 | 4 | 4 | 4 | 4 |
| Antennas [$N_{ant}$] (UL/DL) | 2/4 | 2/4 | 2/4 | 2/8 | 2/8 | 2/8 |
| MIMO Layers [$N_{layers}$] (UL/DL) | 2/4 | 2/4 | 2/4 | 2/4 | 2/4 | 2/4 |
| Modulation Index [$I_{MSC}$] (UL/DL) | 16/28 | 16/28 | 16/28 | 28/27 | 28/27 | 28/27 |

■ Reference cell configuration assumed in subsequent analysis

potentially multiple concurrent frequency bands. Calculations outlined agree well with similar industry led published analysis in [46] and are used in later dimensioning analysis to represent a single RU small cell or distributed MIMO C-RAN deployment.

### B. LATENCY

Unlike fronthaul data rates, the latency requirements (one way delay) of the different lower layer functional splits are constrained by time bound closed loop processes higher in the protocol stack. As the fronthaul interface must support a range of cell configurations, the latency requirement becomes a function of the cell configuration, most notably whether the cell is 4G LTE or 5G NR.

#### 1) 4G LTE

For 4G LTE fronthaul (3GPP option 6 and below) the packet delay constraint is underpinned by the total delay budget of the uplink HARQ (Hybrid Automatic Repeat Request) process which operates at the MAC layer. In LTE, HARQ is asynchronous in downlink and synchronous in the uplink . In uplink HARQ, retransmission for each process occurs at predefined times relative to the initial transmission (every 8 subframes - equivalent to 8 $ms$ or 8 transmission time intervals TTIs). In FDD, retransmission must occur within the 8 $ms$ constraint and therefore the UE must decode its data on subframe $n$, prepare a response and transmit within 4 $ms$ (4 TTI). As the UE must start its ACK/NACK transmission in the subframe $n$ + 4 it nominally has 3 TTIs (3 $ms$) processing time available as in Fig. 3. As a result, a 100 $\mu s$ maximum one-way delay tolerance is typically specified [20] [30] once any processing delay of the HARQ procedure has been factored out. As this processing delay is implementation specific a more relaxed fronthaul delay budget is often quoted between 123 $\mu s$ [13] and 250 $\mu s$ [7] (where 2.5 $ms$ is typically assumed for processing delay leaving 500 $\mu s$ round trip delay or 250 $\mu s$ one-way delay). For the nFAPI split 6 interface, the Small Cell Forum specifies signaling to allow HARQ interleaving and deferral of HARQ buffer emptying, this allows for higher 250$\mu s$ latency fronthaul links to be reliably tolerated.

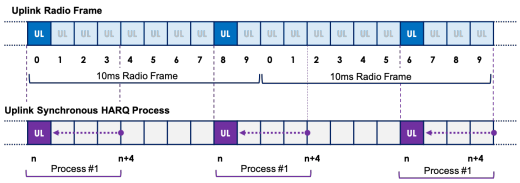


FIGURE 3: Delay Constraints in LTE Fronthaul.

#### 2) 5G NR

In 5G NR, asynchronous (signaled) HARQ is used in the uplink as well as downlink meaning that fronthaul splits at MAC layer and below are no

TABLE 2: Summary of Fronthaul Latency Requirements.

| | eCPRI[22] | O-RAN [39] | IEEE [30] | One-way Delay Requirement | 4G LTE User Plane | 4G LTE Control Plane | 5G NR User Plane | 5G NR Control Plane | Application |
|---|---|---|---|---|---|---|---|---|---|
| High Priority | High25 | High25 | Class 2 | 25$\mu s$ | | | ✓ | | Full NR Ultra-low latency performance |
| | - | High75 | - | 75$\mu s$ | | | ✓ | | Full NR performance with fiber lengths in the 10 km range |
| | High100 | High100 | Class1 /Class2 | 100$\mu s$ | ✓ | | ✓ | | Full E-UTRA or NR performance |
| | High200 | High200 | Class2 | 200$\mu s$ | | | ✓ | | Installations with fiber links lengths in the 40 km range |
| | High500 | High500 | Class2 | 500$\mu s$ | | | ✓ | | Large latency installations |
| Medium | Medium | Medium | Class2 | 1ms | | ✓ | ✓ | ✓ | User Plane (slow), C and M Plane (fast) |
| Low | Low | Low | Class2 | 100ms | | ✓ | | ✓ | C and M Plane (slow) |

Reference cell configuration assumed in subsequent analysis

longer constrained by the HARQ process. For Ethernet based 5G NR fronthaul, the transport latency requirement is instead driven by the next closed loop protocol timing constraint which is the configuration of the response window function in the random access procedure. During network attach, the UE decodes the random access channel (RACH) configuration found in the cell broadcast information. This determines the time, frequency, preamble identity and repetition information to use when initiating the attach procedure (sending of a PRACH preamble) to the gNB (*MSG1*) as in Fig. 4. If *MSG1* is received correctly by the gNB, it transmits a random-access response (RAR) message to the UE (*MSG2*). The UE will monitor the physical downlink control channel (PDCCH) for the RAR message for a defined monitoring period. This monitoring period is set by the *raResponseWindow* parameter in system information block 1 (SIB1) which has a configurable value (defined in number of slots in 5G NR [6]. In 5G NR the subframe length of 1 $ms$ can be divided into 1, 2, 4, 8, 10, 20, 40, 80 slots lasting a maximum of 1 ms or minimum of 12.5 $\mu s$ [4]. As such the configured *raResponseWindow* is defined by the operator's choice of numerology and targeted coverage and mobility of the cell. For a typical 100 MHz carrier running 60 kHz sub carrier spacing as in Table. 1 there are 4 slots per subframe equating to a minimum configurable window size (and one way delay budget) between 250 $\mu s$ and 2 $ms$.

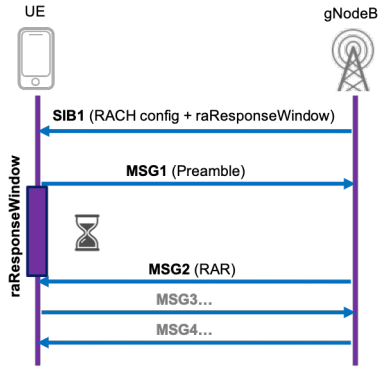


FIGURE 4: Delay Constraints in NR Fronthaul.

To account for the variability in delay budget created by 5G NR specific configurations as well as the HARQ feedback loop constraint in 4G LTE, fronthaul transport specifications such as 802.1CM, O-RAN and eCPRI define a range of latency classes between 25 $\mu s$ for URLLC (5G ultra reliable low latency communication) use cases to 500 $\mu s$ for large latency deployments incorporating longer transport propagation delay or switching delay in multi-hop transport networks.

TABLE 3: Summary of Fronthaul Timing Error Requirements

| Category | Time Error Requirements | | 3GPP Time Alignment Error between Antennas | |
|---|---|---|---|---|
| | Integrated T-TSC[1] | Non-integrated T-TSC | | |
| A+ (relative) | - | 20 $ns$ | 65 ns | e.g. MIMO or Transmission Diversity |
| A (relative) | 60 $ns$ | 70 $ns$ | 130 ns | e.g. FR2 Intra-band contiguous carrier aggregation |
| B (relative) | 190 $ns$ | 200 $ns$ | 260 $ns$ | e.g. FR1 Intra-band contiguous carrier aggregation |
| C (absolute) | 1100 $ns$ [2] | 1100 $ns$ | 3 $\mu s$ | e.g. TDD and dual-connectivity |

Reference cell configuration assumed in subsequent analysis

The control (and management) plane traffic flows for fronthaul splits necessary for scheduling and beamforming commands typically have greater tolerance in the transport delay budget. As these commands are typically vendor specific they are treated with more generalized requirements ranging from between 1 $ms$ for 'fast' to 100 $ms$ for 'slow' control traffic. A summary of Ethernet based fronthaul latency requirements and associated priority classes outlined by the relevant industry specification groups is given in Table. 2.

### C. JITTER/TIMING ERROR

The evolution toward Ethernet based fronthaul means that synchronization information is no longer transmitted by the specific fronthaul protocol (i.e eCPRI, O-RAN or nFAPI) but instead is addressed with existing timing and synchronization protocols such as Synchronous Ethernet (SyncE) or Precision Timing Protocol (PTP). For legacy option 8 fronthaul, synchronous interface protocols such as CPRI specify a 65 $ns$ maximum variation in delay (jitter) of 2 sample periods $Ts$ [20]. This is based on a 20 MHz LTE carrier where the sampling frequency $fs$ is 30.72 MHz. For packet based fronthaul networks the maximum delay variation constraints are fundamentally tied to the timing error budget of the RAN. Existing timing and synchronization protocols such as PTP and associated PTP profiles such as G.8275.1 [35] are utilized to meet the relevant 3GPP time alignment error (TAE) specifications [1], [3]. As such it is the 3GPP feature set supported by the RAN which dictate the TAE and resulting timing accuracy requirements between DU and RU or clustered RUs. There are two distinct timing requirements for the RAN; an absolute time error referenced to a primary reference time clock (PRTC) or telecom grand master (T-GM) clock and a relative time error measured between any two elements in the cluster e.g RUs running telecom time slave clocks (T-TSC) or intermediate telecom boundary clocks (T-BC). The time error budget requirements to meet the 3GPP TAE targets are derived in 802.1CM [30] and presented in Table 3. For the FR1 5G RU example as outlined in Table 1 supporting intra-band contiguous carrier aggregation, the maximum delay variation between elements is 190 $ns$ [34], [39], [22].

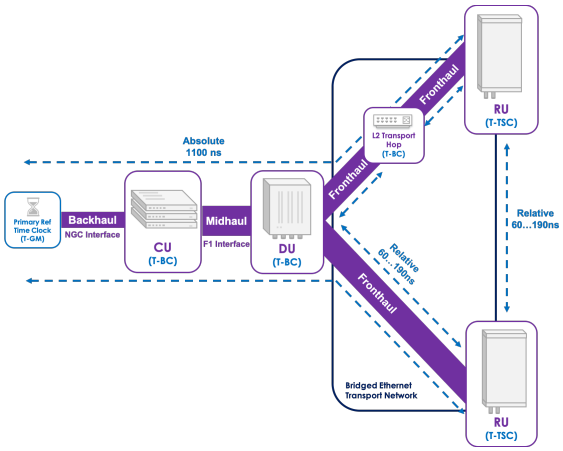


FIGURE 5: Example Timing and Synchronization Fronthaul Architecture (integrated T-TSC).

### D. FRAME LOSS

In bridged Ethernet fronthaul networks the frame loss ratio is specified as the limit which can be tolerated by the interface. As a result the allowable frame loss does not meaningfully characterize the service availability or resulting network

TABLE 4: Summary of Fronthaul Frame Loss Requirements.

| Priority | Application | Frame Loss Ratio |
|---|---|---|
| High (High25 - High500) | User Plane (fast) | $10^{-7}$ |
| Medium | User Plane (slow), C and M Plane (fast) | $10^{-7}$ |
| Low | C and M Plane (slow) | $10^{-6}$ |

Reference cell configuration assumed in subsequent analysis

performance. As with latency requirements, frame loss tolerance is specified per traffic flow (where priority classes are the same as in Table 2) with a common definition and specification across the various standardization groups eCPRI, O-RAN and IEEE - summarized in Table 4. The maximum tolerable frame loss ratio between edge ports of an I/Q based fronthaul data flow for the most stringent 'high' and 'medium' class of service (CoS) is $10^{-7}$. A more relaxed frame loss tolerance of $10^{-6}$ for 'slow' control flows is specified [39].

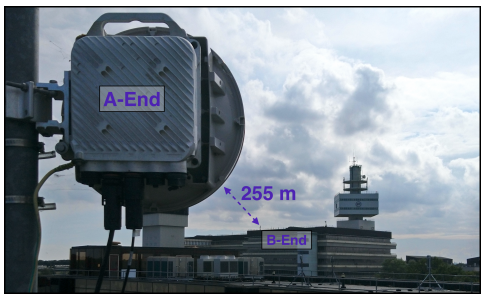


FIGURE 6: E-band Test Bed Transport Link.

## III. EXPERIMENTAL SETUP

### A. FRONTHAUL TEST BED SYSTEM MODEL

In support of the wireless fronthaul feasibility analysis, a wireless fronthaul test bed is built and characterized.The experimental setup / system model is depicted in Fig. 7 where the fronthaul transport link under test is a point-to-point E-band (73.375-75.875 GHz / 83.375-85.875 GHz) mmWave link as shown in Fig. 6. The link can be configured for upto 2 GHz channel bandwidth providing a maximum physical layer data rate of 10 Gbps at 128 QAM modulation. The link spans a 255 m distance between rooftops at BT labs in Martlesham, UK where longer link performance is assessed through modification of the operating modulation.

The RAN aspects of the fronthaul test bed are provided by the open source software libraries of OpenAirInterface5G (OAI5G) [40]. Although not all the industry standardized fronthaul specifications of interest are sufficiently mature and available within the OAI framework at the time of writing, benchmarking of the wireless fronthaul network segment in isolation is considered for subsequent dimensioning and feasibility analysis. Experimentation of the most challenging OAI option 8 fronthaul interface using a low bandwidth 4G eNodeB have been previously reported in [48].

### B. BENCHMARKING RESULTS

The theoretical fronthaul requirements discussed in Section II are first assessed against the capability of the E-band link with a benchmarking exercise of the test bed transport network (TN) outlined in Fig. 7. Each transport performance metric criteria (as outlined in Section II) is assessed with alignment to RFC 2544 [12] test procedures for 0% frame loss and with $\pm$ 10 $ns$ accuracy. In the benchmarking exercise, the test traffic payload is generated using an Ethernet traffic load tester aligned with the OAI fronthaul implementation and broadly equivalent to eCPRI overhead. The Ethernet framing headers accounts for an additional 14 bytes per 1514 byte frame. In the OAI implementation, rather than a standardized RoE or eCPRI Ethertype header, an IP and UDP encapsulation is used accounting for an additional 28 bytes and an available fronthaul data payload of 1472 bytes. The capacity, latency and jitter characteristics of the wireless fronthaul are measured at three different channel bandwidths $BW_{GHz}$ of the E-band radio; 0.5 GHz, 1 GHz and 2 GHz (the maximum possible with the E-band equipment and spectrum band available). The performance expectations of different length links are assessed through manual configuration of each modulation rate supported. Based on the measured results the anticipated performance of

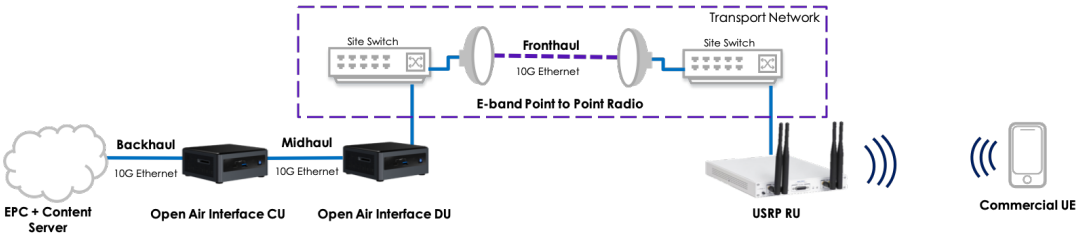


FIGURE 7: Wireless Fronthaul Test Bed Setup

a higher capacity 5 GHz channel is also modeled with the aim of representing the future capability of a D-band or aggregated E+W band transport solution.

### 1) Data Rate Measurements and Modeling

The maximum available capacity measured over the E-band transport link with a 1472 byte fronthaul payload was 9589.9 Mbps as shown in Fig. 8. This was achieved at the highest modulation rate of 128 QAM (7 bits per symbol) and maximum available channel bandwidth of 2 GHz for the equipment under test. The measured capacity for other lower bandwidth and modulation configurations is also presented in Fig. 8. In addition to the measured results, the theoretical capacity for each modulation rate (in bits per symbol $BPS$) and higher channel bandwidths $BW_{GHz}$ representative of future W or D-band systems is calculated from 7 where the data stream coding schemes and coding rates assumed are aligned with ETSI fixed radio system examples [23]. Whilst the coding and overheads assumptions outlined in Table. 5 may not necessarily be representative of all commercially available mmWave transport systems, the modeling calculations, which are also overlaid in Fig. 8, fit well to the measured results providing confidence in the forecast capacities for 5 GHz channels possible in bands above 100 GHz.

$$TN\_Capacity_{Gbps} = (BPS \cdot BW_{GHz}) \cdot RS_{OH} \cdot TC_{OH} \cdot ETH_{OH} \quad (7)$$

In addition to the measured and forecast capacity of the transport link, example data rates for each of the functional splits discussed in Section II are also overlaid in red on Fig. 8. The fronthaul requirements for the 'reference cell' configuration in Table. 1 (a 5G FR1 RU with 100 MHz carrier) serve as reference for later fronthaul dimensioning.

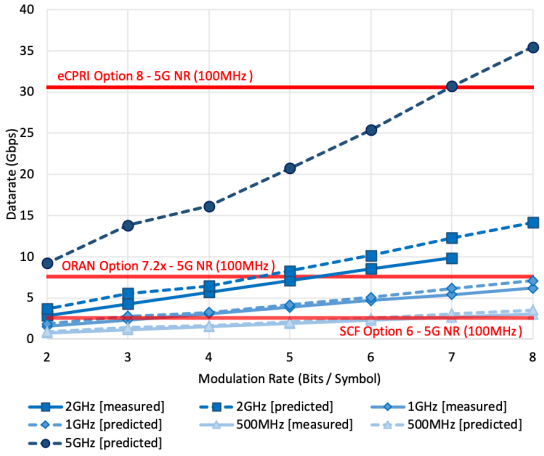


FIGURE 8: Transport Capacity (1472 byte).

### 2) Latency Measurements and Modeling

The latency characteristics of the commercial E-band link are also recorded for a range of modulation schemes and channel bandwidths in Fig. 9. These transport network characteristics also include any delay contribution through the two site switches and represent an ideal deployment where there is no other traffic aggregation, prioritization or queuing present on any of the Ethernet ports in the path. The transport network elements in this particular scenario do not support the ideal end-to-end IEEE time-sensitive network (TSN) protocols which have the to potential to further optimise performance for priority fronthaul traffic flows.

TABLE 5: Wireless Transport Capacity Model Coding and Overhead Assumptions.

| **Transport Link Modulation** | **QPSK** | **8PSK** | **16 QAM** | **32 QAM** | **64 QAM** | **128 QAM** | **256 QAM** |
|---|---|---|---|---|---|---|---|
| PHY Symbol Rate $BPS$ | 2 | 3 | 4 | 5 | 6 | 7 | 8 |
| PHY Coding | RS (255/243) | RS (255/243) | 16TCM-4D (4/3.5) + RS (255/243) | 32TCM-2D (5/4.5) + RS (255/243) | 64TCM-4D (6/5.5) + RS (255/243) | 128TCM-4D (7/6.5) + RS (249/243) | 256TCM-4D (8/7.5) + RS (249/243) |
| Reed-Solomon Overhead $RS_{OH}$ | 0.953 | 0.953 | 0.953 | 0.953 | 0.953 | 0.976 | 0.976 |
| Trellis Coding Overhead $TC_{OH}$ | - | - | 0.875 | 0.900 | 0.917 | 0.929 | 0.938 |
| Ethernet Overhead $ETH_{OH}$ | 0.968 | 0.968 | 0.968 | 0.968 | 0.968 | 0.968 | 0.968 |

The minimum one-way delay measured for a 1472 byte fronthaul payload was of 40.6 $\mu s$ achieved at the highest capacity configuration of 2 GHz and 128 QAM. The measured results demonstrate a clear correlation with the available link capacity allowing a prediction model to be derived for equivalent higher capacity links. A curve fitting approach is used to extrapolate results for the predicted 5 GHz channel because although the latency characteristics are fundamentally a function of the available bandwidth, the queuing, buffer and processing delay contributions of the hardware will be implementation specific and thus not easily modeled for future D-band hardware performance. As a result the latency prediction model in 8 describes the derived function that can be used to predict the latency curve for higher channel bandwidths (namely 5 GHz) - consequently the formulation is based solely on the required channel bandwidth and modulation.

$$TN\_Latency_{\mu s} = (138 \cdot BW_{GHz}^{-0.8}) \cdot BPS^{(0.23 \cdot ln(BW_{GHz}))-0.52}, \quad 0.5 \leq BW_{GHz} \leq 5 \tag{8}$$

The predicted latency characteristics are overlaid with measured results in Fig. 9. The one-way delay threshold for the 'reference cell' configuration in Table 1 and 2 (High 100) is again shown in red for later dimensioning analysis.

### 3) Jitter Measurements and Modeling

The measured jitter characteristics for the E-band link are shown in Fig. 10 where the minimum achievable jitter of 20 $ns$ was measured at the highest capacity configuration. The measured jitter values represent a wireless transport network leg where there is no traffic prioritization or management implemented. In practice, delay variation in the transport network could be optimized through application of TSN Ethernet specifications where effective queue and buffer management could potentially reduce or eliminate jitter at the cost of increased fixed one-way delay [10]. Again, a jitter model is also constructed based on curve fitting of the measurement data of the test bed radio link in order to predict likely jitter characteristics of wider channel solutions. The resulting curve fitting function is outlined in 9. The jitter prediction model shows a good fit to measurement data at higher modulation schemes albeit with reduced accuracy at lower modulation rates with smaller channel sizes.

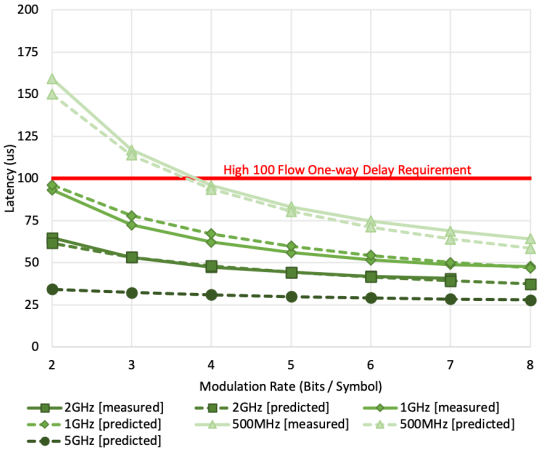


FIGURE 9: Transport Latency (1472 byte).

$$TN\_Jitter_{ns} = (1424 \cdot BW_{GHz}^{-0.7}) \cdot BPS^{(-0.43 \cdot BW_{GHz}) - 0.82}, \quad 0.5 \leq BW_{GHz} \leq 5 \tag{9}$$

The relative timing requirements (Category B) used for the 'reference cell' fronthaul interface as highlighted in Table 3 is also overlaid on Fig. 10 in red. This represents the maximum permissible timing error for a 5G FR1 fronthaul traffic flow (without optimized TSN timing and synchronization support) and is used in the subsequent dimensioning analysis.

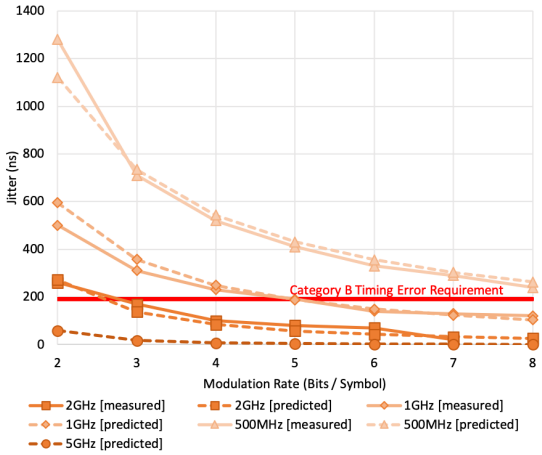


FIGURE 10: Transport Jitter (1472 byte).

## IV. WIRELESS FRONTHAUL DEPLOYMENT OPPORTUNITIES

### A. WIRELESS TRANSPORT LINK BUDGET

To support the performance profiles and predictions in Section III, the link budget for each candidate wireless fronthaul transport band is also modeled. The system configuration assumptions for the wireless transport options are detailed in Table 6. For simplicity we assume a single carrier, single polarization, FDD system in each case. Many configurations are possible in these bands however each follow a 250 MHz channel raster aligned with ITU specifications. For E-band, the maximum channel size currently specified by the ITU is 2 GHz with a duplex spacing of 10 GHz. Assumptions about channel operating frequency and maximum channel bandwidths possible for W-band and D-band are aligned with current industry expectations [26] pending channel arrangement harmonization in these bands [16]. The channel rasters for W and D-band also follow 250 MHz spacing where 2 GHz channel size is assumed for W-band with an FDD duplex separation of 11.55 GHz (sub- channel arrangement 'M' [15]) and 5 GHz for D-band with an FDD duplex spacing of 15.50 GHz (sub-band arrangement 'b/c' [14]).

Other key system parameters that directly influence the total system gain and resulting link budget are the achievable transmit power and antenna gain. For E-band, the transmit power available on commercial solutions such as that utilized in the test bed is in the order of +10 dBm. For W-band the frequency range and channel bandwidths are broadly in line with E-band for which they are expected to be based on similar transistor and fabrication technologies and thus equivalent transmit power. For D-band, literature would suggest that alternative fabrication technologies are more suitable for higher frequencies but equivalent power output is nevertheless achievable [8] and as such the assumed transmit power has been scaled with channel bandwidth accordingly. It remains to be seen where the optimal cost / efficiency point will be for commercial solutions. For antenna gain, the 30 cm 46.6 dBi parabolic antenna used in the test bed environment does not represent a solution suitable for dense urban or street level deployments such as small cell RUs. Advancements in flat panel antenna systems and potential auto-beam alignment techniques offer by compact phased array antennas promise more appropriate solutions albeit with reduced peak gains. As such the link budget analysis assumes antenna gains in the order of 35-40 dBi based on early prototype studies [43] [27].

The minimum received signal level required for each modulation scheme $RSL_{mod}$ is aligned with ETSI TR 101 854 v2.1.1 [23] in (10) when considering the channel bandwidth $B_{MHz}$, typical noise figure $NF$, industrial margin $IM_F$ and theoretical signal-to-noise ratio necessary for the modulation rate bits per symbol $SNR_{mod}$. The resulting link budget calculations in are within 1 dB of the manufacturer quoted specifications for the E-band test bed link and thus a suitable approximation for future commercialized systems operating at W and D band.

TABLE 6: Summary of Wireless Transport System Parameters.

| | E-band | | W-band | | D-band | |
|---|---|---|---|---|---|---|
| | **A-End** | **B-End** | **A-End** | **B-End** | **A-End** | **B-End** |
| Frequency (MHz) | 72125 | 82125 | 95325 | 103125 | 143625 | 158625 |
| Channel Bandwidth (MHz) | 2000 | 2000 | 2000 | 2000 | 5000 | 5000 |
| Water Vapour Attenuation (dB/km) [32] | 0.25 | 0.32 | 0.43 | 0.54 | 1.09 | 1.59 |
| Gaseous Adsorption (dB/km) [32] | 0.20 | 0.06 | 0.03 | 0.04 | 0.02 | 0.02 |
| Polarization | V | V | V | V | V | V |
| Rain Rate 99.99% Availability (mm/hr) | 25 | 25 | 25 | 25 | 25 | 25 |
| Rain Attenuation (dB/km) [33] | 10.62 | 11.30 | 11.90 | 12.07 | 12.51 | 12.74 |
| Tx Radiated Power (dBm) | 10.00 | 10.00 | 10.00 | 10.00 | 6.02 | 6.02 |
| Tx Antenna / BF Gain (dBi) | 40 | 40 | 35 | 35 | 35 | 35 |
| Rx Antenna / BF Gain (dBi) | 40 | 40 | 35 | 35 | 35 | 35 |
| Rx Chain Losses (dB) | 1.00 | 1.00 | 1.00 | 1.00 | 1.00 | 1.00 |
| Rx Noise Figure (dB) | 13.00 | 13.00 | 13.00 | 13.00 | 13.00 | 13.00 |
| Industrial Margin (dB) | 4.00 | 4.00 | 4.00 | 4.00 | 4.00 | 4.00 |
| **Min Rx Sensitivity (dBm)** | **-63.99** | **-63.99** | **-63.99** | **-63.99** | **-60.01** | **-60.01** |
| **Max System Gain (dB)** | **152.99** | **152.99** | **142.99** | **142.99** | **135.03** | **135.03** |

$$RSL_{mod} = -174 + 10 \cdot (\log_{10} B_{MHz}) + NF + IM_F + SNR_{mod} \quad \text{Where}$$
$$SNR_{mod} = 10 \cdot \left(\log_{10}\left(2^{BitsPerSymbol}\right) - 1\right) \tag{10}$$

The environmental conditions necessary to meet a 99.99% atmospheric availability target in the link budget calculations are modeled using ITU atmospheric adsorption modeling recommendations ITU-R P.676-11 [32]. Water vapor attenuation $\gamma_w$ and gaseous (dry air) adsorption $\gamma_o$ contributions in $dB/km$ are calculated based on a representative UK atmospheric pressure of 101.3 $kPa$, a temperature of 15°$C$ and a water vapor density of 7.5$g/m^3$. For peak rainfall losses $\gamma_R$ factored in to the link margin, a 25 $mm/hr$ rain rate in $dB/km$ is assumed (ITU rain zone F for the UK) where calculations are aligned with ITU-R P.838-3 [33] for a vertically polarized, 0° path elevation link. The total path loss calculation at distance $d_{km}$ is given in 11.

$$PL = 32.4 + (20 \cdot (\log B_{MHz})) + (20 \cdot (\log d_{km})) + (d_{km} \cdot (\gamma_w + \gamma_o + \gamma_R)) \tag{11}$$

The resulting path loss profile in terms of total system gain requirements and associated data rate expectations (based on a maximum 256 QAM modulation and minimum QPSK) can be seen in Fig. 11 and 12.

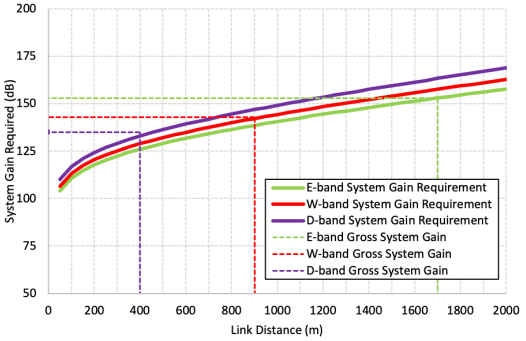


FIGURE 11: System gain requirements for single hop wireless transport.

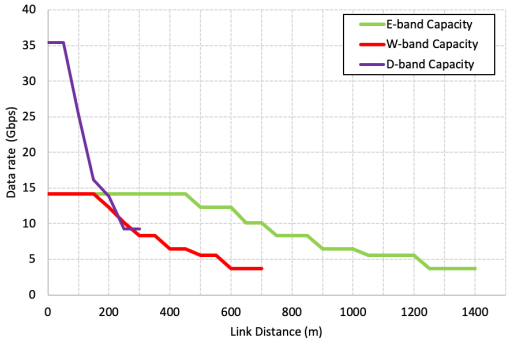


FIGURE 12: System capacity for single hop wireless transport.

### B. REFERENCE CELL DIMENSIONING

To understand the deployment feasibility of wireless fronthaul we combine the performance measurements and predictions from Section III and the link budget analysis from Section IV-A. The cell configuration used in the dimensioning exercise is the 100 MHz 5G cell highlighted in Tables 1, 2 and 3 which aim to be representative of a typical 5G small cell or distributed RU. The performance requirements of the reference cell for each of the standardized functional split interfaces considered (eCPRI option 8, O-RAN option 7.2x and SCF nFAPI option 6) are applied to the link budget capacity capability of Fig. 12.

For each candidate transport band (E, W and D-band) the fronthaul requirements for each split are used to highlight the wireless fronthaul link lengths achievable for the reference cell - Fig. 13, 14 and 15. When considering each of the data rate, latency and jitter requirements it can be seen that only D-band could feasibly support an option 8 fronthaul interface due to capacity constraints of the other bands. While the reference cell employing an option 7.2x or 6 split could be supported on all candidate bands, only D-band could support these interfaces over the full link budget of the system (upto 350 m). The O-RAN option 7.2x split becomes data rate constrained with E-band and W-band after 850 m and 350 m respectively whilst the lower data rate SCF nFAPI option 6 becomes jitter constrained in E-band beyond 1250 m and 550 m in W-band. Although the capacity requirements of an option 8 fronthaul interface demonstrate a limited deployment potential, the operating regions for option 7.2x and 6 in these high frequency transport bands suggest good alignment with dense urban cell deployments seeking to benefit from centralized architectures [49].

## V. SUMMARY AND CONCLUSIONS

In this study the theoretical requirements of competing fronthaul interfaces are assessed against the performance expectations of emerging high frequency transport bands. The aim of this approach is to quantify the deployment opportunity for wireless fronthaul C-RAN deployments in the face of challenging fronthaul performance requirements generally assumed to require ubiq-

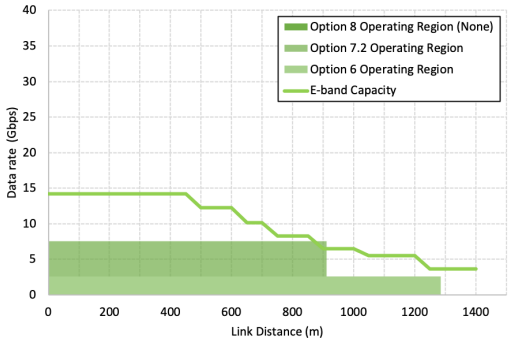


FIGURE 13: Operating regions for reference cell using E-band transport.

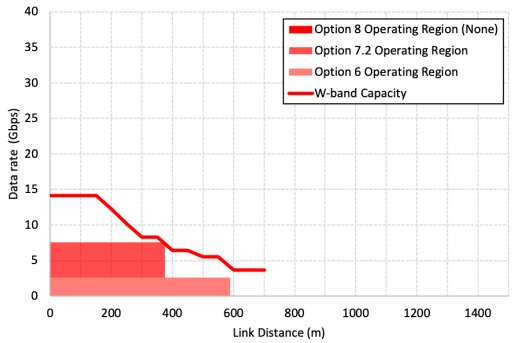


FIGURE 14: Operating regions for reference cell using W-band transport.

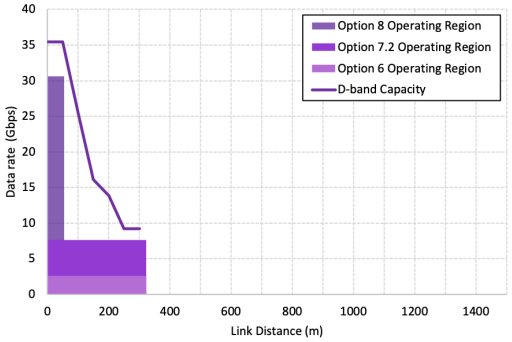


FIGURE 15: Operating regions for reference cell using D-band transport.

uitous fiber transport.

Finding have shown that in spite of the demanding transport requirements imposed by emerging fronthaul interfaces, the anticipated performance of wireless transport systems operating in high mmWave and sub-THz spectrum bands is capable of supporting realistic wireless fronthaul deployments. The capacity requirements for an example 5G small cell with an eCPRI option 8 fronthaul split mean this split is only realizable with large 5 GHz channel bandwidths possible in D-band and even then are only achievable with short link lengths < 100 m. Alternative splits such as O-RAN option 7.2x and SCF nFAPI option 6 show more promise and could be supported on smaller 2 GHz channel bandwidths possible with E and W band where link distances are comparable with urban inter-site distances.

In addition, it is anticipated that future advancements and maturity in wireless transmission systems >100 GHz could further enhance the performance and link lengths achievable in wireless fronthaul transport networks. Advanced radio interface techniques already realized in lower frequency microwave bands including the simultaneous use of multiple carriers, higher order modulation, a second polarization or line-of-sight MIMO techniques promise to double or even quadruple the aggregate link capacities suggested in this work. As a result, it is conceivable that future wireless transport solutions >100 GHz could realistically achieve performance parity with 40 Gbps or 100 Gbps fiber optic solutions over short distances. Such capability, in addition to supporting single RU small cell deployments, could also realize larger multi-sector, multi-carrier macro cell sites.

The findings of this study not only demonstrate the feasibility of the wireless fronthaul concept but highlight a real-world opportunity to evolve the distributed-RAN deployments of today, heavily dependent on lower capacity microwave backhaul, towards more centralized fronthaul orientated architectures using high capacity mmWave and sub-THz transport bands.

## References

[1] 3GPP. *TS 36.104 V17.7.0 Evolved Universal Terrestrial Radio Access (E-UTRA); Base Station (BS) radio transmission and reception*. 2022.

[2] 3GPP. *TS 36.213 V17.3.0 Evolved Universal Terrestrial Radio Access (E-UTRA); Physical layer procedures*. 2022.

[3] 3GPP. *TS 38.104 V17.7.0 NR; Base Station (BS) radio transmission and reception*. 2022.

[4] 3GPP. *TS 38.211 V17.3.0 NR; Physical channels and modulation*. 2022.

[5] 3GPP. *TS 38.214 V17.3.0 NR; Physical layer procedures for data*. 2022.

[6] 3GPP. *TS 38.331 V17.2.0 NR; Radio Resource Control (RRC) protocol specification*. 2022.

[7] 3GPP. *TSG RAN WG3 R3-161813, Transport requirement for CU and DU functional splits options*. 2016.

[8] Ibrahim Kagan Aksoyak et al. "A D-Band Power Amplifier with 15 dBm Psat in 0.13 um SiGe BiCMOS Technology". In: *2022 IEEE 22nd Topical Meeting on Silicon Monolithic Integrated Circuits in RF Systems (SiRF)*. 2022, pp. 5–8. DOI: 10.1109/SiRF53094.2022.9720048.

[9] Isiaka Ajewale Alimi, António Luís Teixeira, and Paulo Pereira Monteiro. "Toward an Efficient C-RAN Optical Fronthaul for the Future Networks: A Tutorial on Technologies, Requirements, Challenges, and Solutions". In: *IEEE Communications Surveys and Tutorials* 20.1 (2018), pp. 708–769. DOI: 10.1109/COMST.2017.2773462.

[10] Mahmoud Bahnasy, Halima Elbiaze, and Catherine Truchan. "CPRI over Ethernet: Towards fronthaul backhaul multiplexing". In: *2018 15th IEEE Annual Consumer Communications and Networking Conference (CCNC)*. 2018, pp. 1–7. DOI: 10.1109/CCNC.2018.8319220.

[11] Jens Bartelt et al. "Fronthaul and backhaul requirements of flexibly centralized radio access networks". In: *IEEE Wireless Communications* 22.5 (2015), pp. 105–111. DOI: 10.1109/MWC.2015.7306544.

[12] *Benchmarking Methodology for Network Interconnect Devices*. RFC 2544. Mar. 1999. DOI: 10.17487/RFC2544. URL: https://www.rfc-editor.org/info/rfc2544.

[13] S. Bjømstad, D. Chen, and R. Veisllari. "Handling Delay in 5G Ethernet Mobile Fronthaul Networks". In: *2018 European Conference on Networks and Communications (EuCNC)*. 2018, pp. 1–9. DOI: 10.1109/EuCNC.2018.8442755.

[14] CEPT. *ECC Recommendation (18)01 - Radio frequency channel/block arrangements for Fixed Service systems operating in the bands 130-134 GHz, 141-148.5 GHz, 151.5-164 GHz and 167-174.8 GHz*. 2018.

[15] CEPT. *ECC Recommendation (18)02 - Radio frequency channel/block arrangements for Fixed Service systems operating in the bands 92-94 GHz, 94.1-100 GHz, 102-109.5 GHz and 111.8-114.25 GHz*. 2018.

[16] CEPT. *ECC Report 282 - Point-to-Point Radio Links in the Frequency Ranges 92-114.25 GHz and 130-174.8 GHz*. 2018.

[17] Juergen Cezanne et al. "Design of Wireless Fronthaul With mmWave LOS-MIMO and Sample-Level Coding for O-RAN and Beyond 5G Systems". In: *IEEE Open Journal of the Communications Society* (2023), pp. 1–1. DOI: 10.1109/OJCOMS.2023.3308713.

[18] Chia-Yu Chang et al. "FlexCRAN: A flexible functional split framework over ethernet fronthaul in Cloud-RAN". In: *2017 IEEE International Conference on Communications (ICC)*. 2017, pp. 1–7. DOI: 10.1109/ICC.2017.7996632.

[19] Divya Chitimalla et al. "5G fronthaul-latency and jitter studies of CPRI over ethernet". In: *Journal of Optical Communications and Networking* 9.2 (2017), pp. 172–182. DOI: 10.1364/JOCN.9.000172.

[20] CPRI Cooperation. *CPRI Specification V7.0*. 2015. URL: http://www.cpri.info/spec.html.

[21] CPRI Cooperation. *eCPRI Specification V2.0*. 2019. URL: http://www.cpri.info/spec.html.

[22] CPRI Cooperation. *eCPRI Transpot Requirements V1.2*. 2018. URL: http://www.cpri.info/spec.html.

[23] ETSI. *TR 101 854 v2.1.1 Fixed Radio Systems; Point-to-point equipment; Derivation of receiver interference parameters useful for planning fixed service point-to-point systems operating different equipment classes and/or capacities*. 2019.

[24] ETSI mWT. *5G Wireless Backhaul/X-Haul*. 2018. URL: https://www.etsi.org/committee/1426-mwt.

[25] ETSI mWT ISG. *Evolution of Fixed Services for Wireless Backhaul of IMT 2020 / 5G*. 2019. URL: https://www.itu.int/en/ITU-R/study-groups/workshops/fsimt2020/Pages/default.aspx.

[26] ETSI, mWT ISG. *Analysis of Spectrum, License Schemes and Network Scenarios in the D-band*. 2018. URL: https://www.etsi.org/committee/1426-mwt.

[27] Mario G. L. Frecassetti et al. "D-Band Backhaul and Fronthaul Solutions for 5G Radio Access Network". In: *2022 52nd European Microwave Conference (EuMC)*. 2022, pp. 772–775. DOI: 10.23919/EuMC54642.2022.9924325.

[28] Chih-Lin I et al. "Recent Progress on C-RAN Centralization and Cloudification". In: *IEEE Access* 2 (2014), pp. 1030–1039. DOI: 10.1109/ACCESS.2014.2351411.

[29] Nagwa Ibrahim, Ashraf A. Eltholth, and Magdy S. El-Soudani. "Hybrid FSO/mmWave based Fronthaul C-RAN Optimization for Future Wireless Communications". In: *2020 29th Wireless and Optical Communications Conference (WOCC)*. 2020, pp. 1–6. DOI: 10.1109/WOCC48579.2020.9114921.

[30] "IEEE Standard for Local and metropolitan area networks – Time-Sensitive Networking for Fronthaul". In: *IEEE Std 802.1CM-2018* (2018), pp. 1–62. DOI: 10.1109/IEEESTD.2018.8376066.

[31] "IEEE Standard for Radio over Ethernet Encapsulations and Mappings". In: *IEEE Std 1914.3-2018* (2018), pp. 1–77. DOI: 10.1109/IEEESTD.2018.8486937.

[32] ITU-R. *P.676-11 Attenuation by atmospheric gases*. 2016.

[33] ITU-R. *P.838-3 Specific attenuation model for rain for use in prediction methods*. 2005.

[34] ITU-T. *G.8271 Time and phase synchronization aspects of telecommunication networks*. 2020.

[35] ITU-T. *G.8271.1 Precision time protocol telecom profile for phase/time synchronization with full timing support from the network*. 2020.

[36] Meilong Jiang et al. "Wireless Fronthaul for 5G and Future Radio Access Networks: Challenges and Enabling Technologies". In: *IEEE Wireless Communications* 29.2 (2022), pp. 108–114. DOI: 10.1109/MWC.003.2100482.

[37] Ping-Heng Kuo and Alain Mourad. "Millimeter wave for 5G mobile fronthaul and backhaul". In: *2017 European Conference on Networks and Communications (EuCNC)*. 2017, pp. 1–5. DOI: 10.1109/EuCNC.2017.7980750.

[38] Line M. P. Larsen, Aleksandra Checko, and Henrik L. Christiansen. "A Survey of the Functional Splits Proposed for 5G Mobile Crosshaul Networks". In: *IEEE Communications Surveys Tutorials* 21.1 (2019), pp. 146–172. DOI: 10.1109/COMST.2018.2868805.

[39] O-RAN Alliance. *Open Xhaul Transport Working Group 9 - Xhaul Transport Requirements v01.00*. 2021. URL: https://o-ran.org/specifications.

[40] Open Air Interface Software Alliance. *Open Air Interface*. 2022. URL: https://openairinterface.org.

[41] Veronica Quintuna Rodriguez et al. "Cloud-RAN functional split for an efficient fronthaul network". In: *2020 International Wireless Communications and Mobile Computing (IWCMC)*. 2020, pp. 245–250. DOI: 10.1109/IWCMC48107.2020.9148093.

[42] Mark J. Roldan, Phillip Leithead, and Jane Mack. "Experiments and results of a mmW transport platform to enable 5G cloud RAN lower layer splits". In: *2018 IEEE Long Island Systems, Applications and Technology Conference (LISAT)*. 2018, pp. 1–6. DOI: 10.1109/LISAT.2018.8378032.

[43] G. Roveda and M. Costa. "Flexible Use of D Band Spectrum for 5G Transport: a Research Field Trial as Input to Standardization". In: *2018 IEEE 29th Annual International Symposium on Personal, Indoor and Mobile Radio Communications (PIMRC)*. 2018, pp. 800–804. DOI: 10.1109/PIMRC.2018.8580825.

[44] Muhammad Usman Sheikh et al. "X-Haul Solutions for Different Functional Split Options Using THz and Sub-THz Bands". In: *Proceedings of the 20th ACM International Symposium on Mobility Management and Wireless Access*. MobiWac '22. Montreal, Quebec, Canada: Association for Computing Machinery, 2022, pp. 47–53. ISBN: 9781450394802. DOI: 10.1145/3551660.3560921.

[45] Small Cell Forum. *5G nFAPI Specifications - SCF225.3.0*. 2022. URL: https://scf.io.

[46] Small Cell Forum. *DARTs - An Analysis Tool for Disaggregated RAN Transport - SCF247.0.1*. 2023. URL: https://scf.io.

[47] Alexandru Stancu, Alexandru Vulpe, and Simona Halunga. "Evaluation of a Wireless Transport Network Emulator Used for SDN Applications Development". In: *IEEE Access* 6 (2018), pp. 15870–15883. DOI: 10.1109/ACCESS.2018.2815844.

[48] Dave Townend et al. "Toward Wireless Fronthaul for Cloud RAN Architectures". In: *2023 IEEE Wireless Communications and Networking Conference (WCNC) (IEEE WCNC 2023)*. Glasgow, United Kingdom, Mar. 2023.

[49] Dave Townend et al. "Urban Wireless Multi-hop x-Haul for Future Mobile Network Architectures". In: *ICC 2022 - IEEE International Conference on Communications*. 2022, pp. 1883–1887. DOI: 10.1109/ICC45855.2022.9838366.

[50] Jun Shan Wey and Junwen Zhang. "Passive Optical Networks for 5G Transport: Technology and Standards". In: *Journal of Lightwave Technology* 37.12 (2019), pp. 2830–2837. DOI: 10.1109/JLT.2018.2856828.

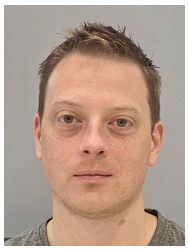

DAVE TOWNEND received the M.Eng degree in wireless communication engineering from Loughborough University, U.K., in 2007 and is currently a Wireless Research Manager at BT Laboratories. He is currently pursuing a Ph.D. degree with the School of Computer Science and Electronic Engineering at the University of Essex, U.K., and is a Chartered Engineer and a Member of the IET. His research interests include high frequency propagation, mobile network deployment modeling and wireless backhaul.

RYAN HUSBANDS received the B.Sc. degree in electronics and mathematics from the University of the West Indies, Cave Hill, Barbados, in 2011. He acquired the M.Sc. degree in wireless communication and signal processing, and the Ph.D. degree in electronic engineering, specialising in massive MIMO, from the University of Kent, in 2012 and 2018 respectively. In 2019, he joined BT - Wireless Research Team as a Specialist Research Professional based at BT Laboratories, Martlesham, U.K. His current research interests include modeling, performance analysis and optimization of wireless communication systems, with interests in vRAN, massive MIMO, RF propagation, antenna arrays, and 4G/5G along with future radio access (FRA) deployments.

STUART D. WALKER received the B.Sc. (Hons) degree in physics from Manchester University, U.K., in 1973, the M.Sc. degree in telecommunications systems and Ph.D. degree in electronics from Essex University, Colchester, U.K., in 1975 and 1981 respectively. From 1981-82, he was a post-doctoral research assistant at Essex University. From 1982-87, he was a research scientist at BT Laboratories, and from 1987-88 he was promoted to Group Leader in Submarine Systems Design. He joined Essex University in 1988 as a Senior Lecturer, and was promoted to Reader in 2002 and to Full Professor in 2004. At Essex University, he manages a laboratory concerned with all aspects of Access Networks: The Access Networks Group (ANG).

ANDY SUTTON is a Principal Network Architect in BT's Architecture and Technology Strategy team where he is responsible for radio access network (RAN) architecture evolution and mobile xhaul strategy. Andy holds an M.Sc. in mobile communications from the University of Salford and has 35 years of experience within the telecommunications industry. His research interests include distributed and centralised RAN architectures, optical and wireless transmission systems and mission critical network design and optimisation. Andy holds the post of Visiting Professor at the University of Liverpool and University of Salford, he's a Chartered Engineer and holds Fellowships from the IET, ITP and BCS. Andy sits on the editorial board of the Institute of Telecommunications Professionals Journal and has co-authored four books on telecommunications topics.